



# A study of the material loss and other processes involved during annealing of GaN at growth temperatures

M.A. Rana <sup>a,\*</sup>, T. Osipowicz <sup>a</sup>, H.W. Choi <sup>b</sup>, M.B.H. Breese <sup>a</sup>, S.J. Chua <sup>b</sup>

<sup>a</sup> Department of Physics, Center for Ion Beam Applications, National University of Singapore, 2 Science Drive 3, Singapore 117542, Singapore

<sup>b</sup> Department of Electrical Engineering, Center for Optoelectronics, National University of Singapore, Singapore 119260, Singapore

Received 12 July 2003; in final form 28 August 2003

## Abstract

Rutherford backscattering spectrometry (RBS) was performed on GaN layers grown on sapphire and annealed at temperatures between 500 and 1100 °C. Protons of energy 2 MeV were used for nanoscale depth-resolved RBS measurements. The simulation package SIMNRA was used to extract quantitative information from RBS results. Our results describe quantitatively the complete evaporation of GaN surface layers followed by partial evaporation of gallium and nitrogen atoms from successive layers along with incorporation of oxygen from the ambient during annealing. The formation of micron-sized islands or terraces on GaN surface during annealing has been explained using RBS and atomic force microscopy results.

© 2003 Published by Elsevier B.V.

## 1. Introduction

Gallium nitride and related alloys are photonic materials with a tremendous range of applications in light emitting diodes (LEDs), laser diodes (LDs), photo-detectors and high temperature devices. Such devices are critical components of full-color displays, compact disk (CD) read/write systems, high-resolution printing and underwater communications [1–5]. Recently, gallium nitride based nanowires and nanorods are found to be

useful for future nanoscale electronic and optoelectronic devices [6,7].

One of the important processes involved in the fabrication of GaN devices is high temperature annealing, which is used to remove the damage produced during earlier fabrication processes. The development of high conductivity p-GaN was a long-standing issue in the fabrication of GaN based devices. This problem was solved using post growth annealing. It is found that annealing process removes hydrogen by breaking Mg–H complexes in p-GaN [8,9], which are considered to be responsible for the passivation of Mg, the shallowest available p-type dopant in GaN. However, GaN decomposes during annealing above a certain temperature. An understanding of the annealing

\* Corresponding author. Fax: +65-67776126.

E-mail address: [scip0229@nus.edu.sg](mailto:scip0229@nus.edu.sg) (M.A. Rana).

of GaN at temperatures used for epitaxial or buffer layer growth is also useful in improving growth conditions. A number of authors [10–17] have reported annealing results of gallium nitride. Among them, Vartuli et al. [17] described surface degradation of III–V nitrides, including GaN, using Auger electron spectroscopy, scanning electron microscopy and AFM. Previously published results on annealing of GaN along with surface protection procedures are given in a comprehensive review by Pearton et al. [18], which covers all the issues involved during fabrication of GaN devices. Despite these investigations, the picture is not complete yet as quantitative measurements of evaporation and depth dependence of decomposition have not been explored completely.

We used 2 MeV proton backscattering to characterize the processes (e.g., evaporation, absorption and change of thickness etc.) induced in GaN during annealing. AFM measurements are combined with nanoscale depth resolved RBS results to explain the properties of altered new surface-region formed after annealing. It is the first study, up to our knowledge, which gives the quantitative analysis of material loss and stoichiometric changes induced in GaN with the depth resolution of better than 20 nm during annealing experiments performed over a wide range of temperatures 500–1100 °C.

## 2. Experimental

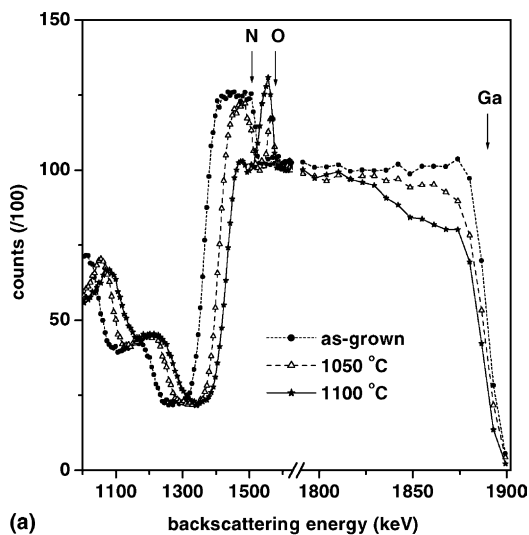
An epitaxial GaN film of thickness 3  $\mu\text{m}$  was grown in an EMCORE D125 metal organic chemical vapor deposition (MOCVD) reactor on a sapphire (0001) substrate with a 25 nm thick low temperature buffer layer sandwiched in between. A number of samples, each of  $5 \times 5 \text{ mm}^2$  area, were cleaved from a GaN wafer and were subjected to rapid thermal annealing at temperatures between 500 and 1100 °C for a time interval of 60 s in flowing nitrogen. The sample temperature was maintained within  $\pm 5$  °C from the set temperature during annealing of all the samples. RBS measurements were carried out using the 3.5 MeV Singletron accelerator at Center for Ion Beam Applications, National University of Singapore.

The backscattered protons were detected using a semiconductor surface barrier detector of resolution 13 keV and an area of  $50 \text{ mm}^2$ . The detector was located at a scattering angle of  $160^\circ$ . The total beam fluence used for each measurement was 5–10  $\mu\text{C}$ . AFM measurements were also carried out on the same as-grown and annealed GaN samples using the tapping mode.

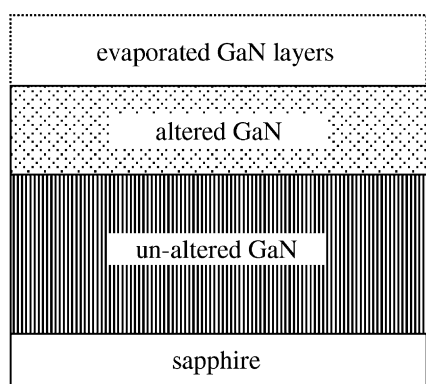
## 3. Results and discussion

Fig. 1a shows 2 MeV proton backscattering spectra from as-grown and annealed GaN samples. Two effects are quite clear from this figure. Firstly, the shift of the low energy edge of the gallium signal, which appears between 1300 and 1900 keV. This is unambiguously recognizable because there is a relatively large gallium edge overlapped with the weak nitrogen signal. It is interpreted as a reduction of GaN thickness. The other effect is a stoichiometric change in the near-surface region after partial decomposition of GaN layers. This change in stoichiometry is caused by the evaporation of gallium and nitrogen atoms and incorporation of oxygen from the ambient where it was present as an impurity during high temperature anneals. These annealing effects are shown in Fig. 1b schematically.

From backscattering spectra, shown in Fig. 1a, it is difficult to see changes in the different species (Ga, N and O) in the GaN film after annealing due to the overlapping of backscattering signals from different species. We have fitted the experimental data in Fig. 1a using the simulation code SIM-NRA [19]. As an example, experimental and simulated proton backscattering spectra are shown in Fig. 2 in case of the GaN sample annealed at 1050 °C. Similarly, simulation was performed for all samples to separate backscattering signals of different species. Separated backscattering signals of gallium, nitrogen and oxygen are shown in Figs. 3a–c, respectively. Fit error in all regions of spectra for data of all the samples is less than 3%. Considering Figs. 3a and b, we can compare the effects of high temperature on the gallium and nitrogen sub-lattices. These figures show quantitatively that high temperature induced changes in



(a)



(b)

Fig. 1. (a) Backscattering spectra using 2 MeV protons from annealed GaN samples. Vertical arrows show the positions at which signals from corresponding elements at the surface are expected to appear. Only selected spectra are shown to avoid overlapping. Lines are drawn to guide the eye. (b) Schematic diagram showing different regions observed in annealed GaN samples. The thickness of these regions can be seen in Figs. 3 and 5.

the gallium lattice are less dramatic than found in the nitrogen lattice. The altered surface-region is severely depleted of nitrogen and in the case of the sample annealed at 1100 °C, a 100 nm deep sub-surface-region is almost free of nitrogen. In this surface layer, oxygen incorporation is observed. The stoichiometry of the 100 nm surface layer of the annealed GaN samples as determined using a 2 MeV proton beam is given in Table 1.

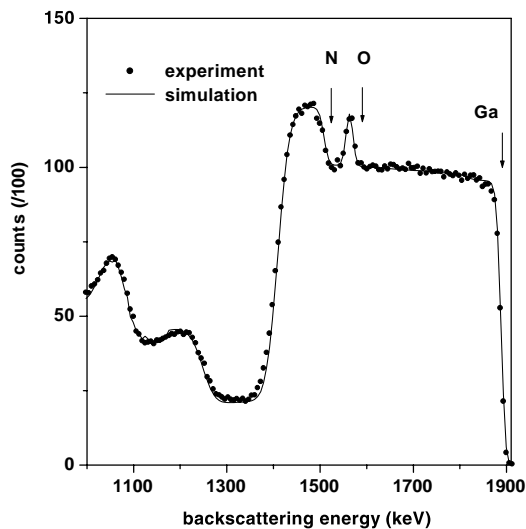
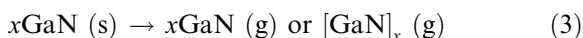
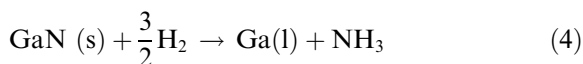


Fig. 2. Experimental and simulated (SIMNRA [19]) proton backscattering spectra in case of GaN sample annealed at 1050 °C.

The modes available for material loss from GaN during annealing include [20–23],



The formation of a Ga-rich surface and gallium droplets [24] on a GaN surface during annealing can be enhanced by the presence of hydrogen, incorporated during growth, through a reaction reported by Morimoto [21],



The results given in Table 1 show that mode of material loss is dominated by the reaction given in Eq. (2) due to observed preferential loss of nitrogen during high temperature annealing. After decomposition of GaN followed by incorporation of oxygen, the altered surface-layer becomes a mixture of gallium metal islands or droplets, gallium oxide (preferably  $\text{Ga}_2\text{O}_3$ ) and gallium oxynitride with components ratio depending upon the annealing temperature. The chemical reactions for the formation of  $\text{Ga}_2\text{O}_3$  and gallium oxynitride are [25,26],

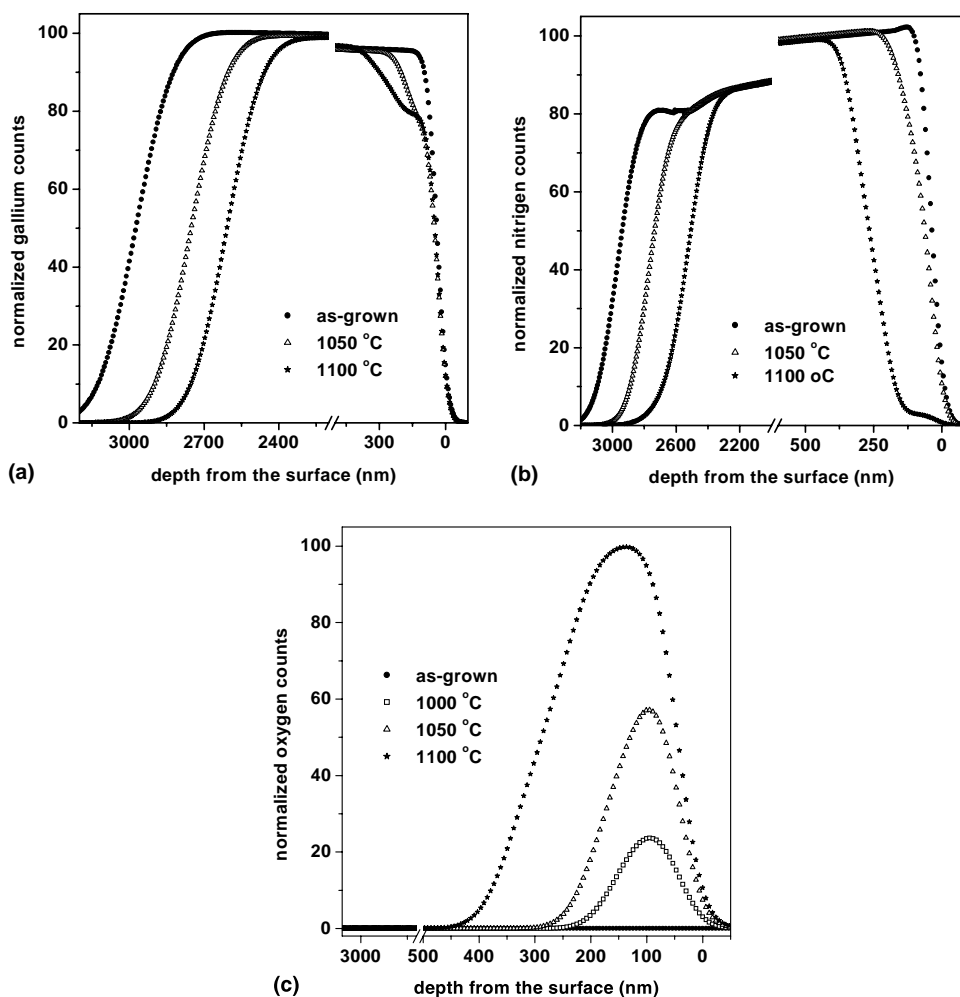
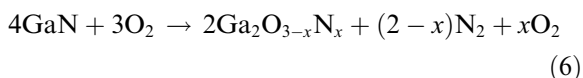
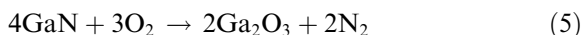


Fig. 3. Depth profiles of gallium (a), nitrogen (b) and oxygen (c) backscattering signal from annealed GaN as determined by fitting the experimental backscattering data, shown in Fig. 1a, with the simulation code SIMNRA [19]. The gap between the backscattering signals at the edges of broken region in each case is due to the change in backscattering cross section of penetrating protons from respective atoms.



In the 1100 °C annealed sample, the ratio of gallium to oxygen is approximately 2:3, with a very small percentage of nitrogen which suggests that most of the 100 nm surface layer in this case is probably  $\text{Ga}_2\text{O}_3$ . In contrast, the stoichiometry of 1000 and 1050 °C annealed samples suggests the presence of metallic gallium, GaN,  $\text{Ga}_2\text{O}_3$  and

gallium oxynitride ( $\text{Ga}_2\text{O}_{3-x}\text{N}_{(2/3)x}$  [25] or  $\text{GaO}_x\text{N}_{1-x}$  [26]).

It is observed that gallium loss becomes appreciable only at temperatures beyond 1000 °C. The mechanism of gallium loss in our experiments can be attributed to the reaction initially studied by Frosch and Thurmond [27] which involves the gallium liquid and gallium oxide produced during as initial products,

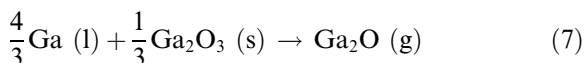


Table 1  
Composition of 100 nm surface layer of as-grown and annealed GaN samples determined using a 2 MeV proton beam back-scattering

Annealing temperature (°C)	Ga (%)	N (%)	O (%)
As-grown	50	50	–
500–800	50	50	–
900	47	43	10
1000	45	29	26
1050	42	25	33
1100	38	4	58

The above reaction explains the mechanism of gallium loss at temperatures (1000–1100 °C) much lower than its boiling temperature.

AFM images in Fig. 4 show formation of micron-sized islands or terraces in GaN samples, which are annealed at temperatures higher than 1000 °C. The size of the islands increases with the annealing temperature. The stoichiometry of the annealed samples, given in Table 1, suggests that these islands might be Ga metal droplets or Ga<sub>2</sub>O<sub>3</sub> poly-crystallites, which increase their size by coalescence due to the increase of diffusion at high temperatures. Fig. 5 shows RMS surface roughness measured using AFM and the thickness of altered region determined by RBS as a function of annealing temperature. The surface roughness and the width of the altered region show similar dependences on annealing temperature. This supports the idea that nitrogen and gallium are evaporated after decomposition at high temperature followed by incorporation of oxygen from the ambient, creating the potential for formation of new phases as Ga<sub>2</sub>O<sub>3</sub> and gallium oxynitride.

#### 4. Conclusions

Complete evaporation of GaN surface layers followed by the alteration of the new surface-region is observed at temperatures, which are important for growth and processing of GaN. The reduction in the thickness of GaN thin layers due to the material loss and the stoichiometry of the altered surface-region after annealing have been determined quantitatively by fitting the experi-

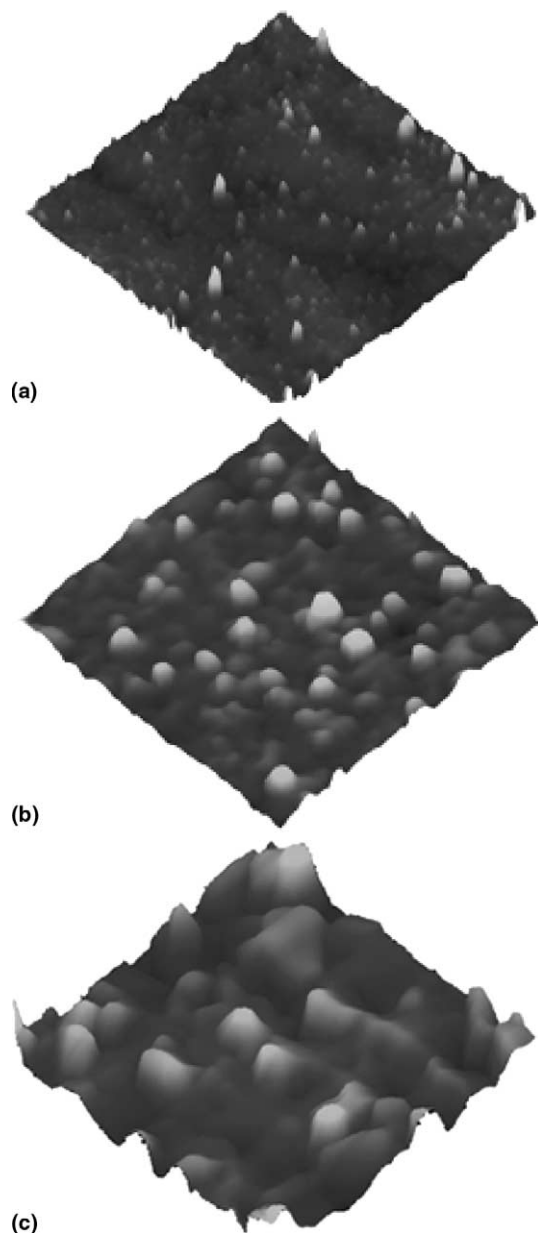


Fig. 4. AFM images of (a) as-grown, and annealed GaN at temperatures of (b) 1050 °C and (c) 1100 °C. All images are over an area of  $4 \times 4 \mu\text{m}^2$  with a full-scale height of (a) 60 nm, (b) 500 nm and (c) 800 nm.

mental data with a fit error of less than 3%. These quantitative results have been used to explain the processes involved during evaporation and stoichiometric changes. The depth of the altered sur-

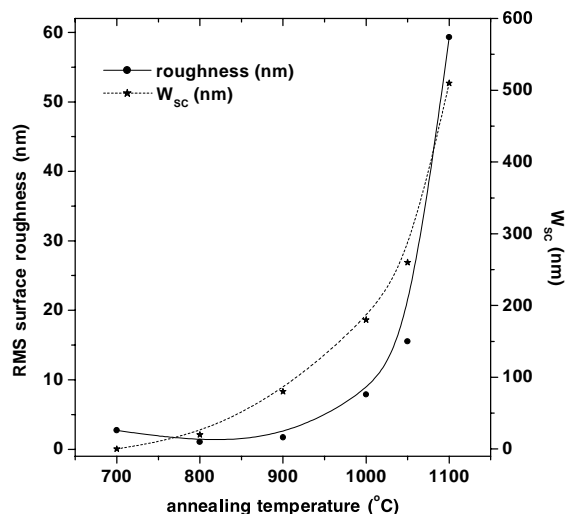


Fig. 5. RMS roughness of annealed GaN samples using AFM and the depth of the altered surface-region ( $W_{sc}$ ) using RBS as a function of annealing temperature.

face-region measured using RBS is found to have a relationship with AFM results of surface roughness. Combined RBS and AFM results explain the formation of micron-sized islands or terraces on GaN surface during annealing. Our nanoscale depth resolution results are useful for further development of fabrication procedure of GaN based conventional and nanoscale devices.

## References

- [1] S. Nakamura, *Science* 281 (1998) 956.
- [2] O. Manasreh, *III-Nitride Semiconductors: Electrical, Structural and Defect Properties*, Elsevier Science, Amsterdam, 2000.
- [3] X. Duan, C.M. Lieber, *J. Am. Chem. Soc.* 122 (2000) 188.
- [4] F.A. Ponce, D.P. Bour, *Nature* 386 (1997) 35.
- [5] S. Nakamura, G. Fasol, *The Blue Laser Diode: GaN Based Light Emitters and Lasers*, Springer-Verlag, Berlin, 1997.
- [6] Y. Huang, X. Duan, C.M. Lieber, *Nano Lett.* 2 (2002) 101.
- [7] W. Han, S. Fan, Q. Li, Y. Hu, *Science* 277 (1997) 1287.
- [8] F.A. Rebroredo, S.T. Pantelides, *Phys. Rev. Lett.* 82 (1999) 1887.
- [9] J. Neugebauer, C. Van de Walle, *Phys. Rev. Lett.* 75 (1995) 4452.
- [10] T. Mattila, R.M. Nieminen, *Phys. Rev. B* 54 (1996) 166676.
- [11] C.H. Park, D.J. Chadi, *Phys. Rev. B* 55 (1997) 12995.
- [12] C.F. Lin, H.C. Cheng, C.C. Chang, G.C. Chi, *J. Appl. Phys.* 88 (2000) 6515.
- [13] J.C. Zolper, R.G. Wilson, S.J. Pearton, R.A. Stall, *Appl. Phys. Lett.* 68 (1996) 1945.
- [14] H.W. Choi, S.J. Chua, A. Raman, J.S. Pan, A.T.S. Wee, *Appl. Phys. Lett.* 77 (2000) 795.
- [15] S.J. Pearton, H. Cho, J.R. LaRoche, F. Ren, R.G. Wilson, J.W. Lee, *J. Appl. Phys.* 75 (1999) 2939.
- [16] M.A. Rana, T. Osipowicz, H.W. Choi, M.B.H. Breese, F. Watt, S.J. Chua, *Appl. Phys. A* 77 (2003) 103.
- [17] C.B. Vartuli, S.J. Pearton, C.R. Abernathy, J.D. MacKenzie, E.S. Lambers, J.C. Zolper, *J. Vac. Sci. Technol. B* (1996) 3523.
- [18] S.J. Pearton, J.C. Zolper, R.J. Shul, F. Ren, *J. Appl. Phys.* 86 (1999) 1.
- [19] M. Mayer, *SIMNRA Users Guide*, Report IPP 9/113, Max-Planck-Institut für Plasmaphysik, Garching, Germany, 1997–2001.
- [20] D.D. Koleski, A.E. Wickenden, R.L. Henry, J.C. Culbertson, M.E. Twigg, *J. Cryst. Growth* 223 (2001) 466.
- [21] Y. Morimoto, *J. Electrochem. Soc.* 121 (1974) 1383.
- [22] Z.A. Munir, A.W. Searcy, *J. Chem. Phys.* 42 (1965) 4223.
- [23] R. Groh, G. Gery, L. Bartha, J.I. Pankove, *Phys. Stat. Sol. A* 26 (1974) 353.
- [24] D.D. Koleske, A.E. Wickenden, R.L. Henry, M.E. Twigg, J.C. Culbertson, R.J. Gorman, *Appl. Phys. Lett.* 73 (1998) 2018.
- [25] D. Kisailus, J.H. Choi, F.F. Lange, *J. Mater. Res.* 17 (2002) 2540.
- [26] H. Kim, N.M. Park, J.S. Jang, S.J. Park, H. Hwang, *Electrochem. Solid State Lett.* 4 (2001) G104.
- [27] C.J. Frosch, C.D. Thurmond, *J. Phys. Chem.* 66 (1962) 877.